Acta Acustica 2022, **6**, 35

https://doi.org/10.1051/aacus/2022027

Available online at:
https://acta-acustica.edpsciences.org

REVIEW ARTICLE OPEN ACCESS

Excitation of pipe bending modes by internal pressure: A phenomenon present in refrigerators with skin condenser

Ricardo Luís Schaefer[1,2,*] and Arcanjo Lenzi[1]

[1] Acoustics and Vibration Laboratory, Department of Mechanical Engineering, Federal University of Santa Catarina, 88040-900 Florianópolis, Brazil
[2] Center of Engineering and Exact Sciences, State University of Western Paraná, 85819-110 Foz do Iguaçu, Brasil

Received 2 November 2021, Accepted 1 July 2022

Abstract – The concept of skin condenser refrigerators has been increasingly explored for its capacity to provide a larger internal cabinet volume. However, the discharge pulsation of the cooling gas has become a significant source of noise because it directly excites the cabinet. This paper analyzes the mechanisms of cabinet vibration excitation by gas pulsation in the condenser tubes. Initial tests were performed with vibration measurements on a refrigerator and on segments of the cabinet excited by pulsation only. The results showed that bending modes of cabinet segments were excited by the pulsation in the condenser tube. A theoretical analysis showed that asymmetry in the condenser tube cross section is responsible for bending moment generation and numerical evaluations confirmed this effect for different types of asymmetries.

Keywords: Vibration, Noise, Refrigerator, Pulsation, Skin condenser

1 Introduction

Household appliances linked to food are indispensable equipment in modern life. Noise related aspects can be considered as major inconveniences, as they are related to the consumers well being and satisfaction [1].

Cooling equipments have different operation regime than other household appliances because in order to maintain the desired temperature they operate at any time [1]. Thus, they have high annoying pontential, since the compressor can be started in moments of silence or when the users are performing activities that require concentration [2].

Refrigerators have several noise sources linked to the refrigeration system. The main ones are compressor, fan and the expansion device, which are considered primary noise sources. Among them, the pressure pulsation in the discharge line [3] is caused by reciprocating compressors that, due to the nature of their operation, produce intermittent pressure pulses. The pulsating characteristics of gas discharge generates a spectrum composed of harmonics, which can excite the natural modes of the piping [4] and refrigerator cabinet. When these harmonics coincide or have frequency close to some structural resonance, vibration will be excited, generating noise.

Skin condenser refrigerators combine aesthetic improvements and increased usable internal space [5, 6]. Unlike external condensers, which are connected via clips, the skin condenser is installed inside the enclosure, making direct contact between the condenser tube and the enclosure, constituting a favorable situation for the transmission of vibratory energy to the cabinet.

Direct contact of the tube with the outer plate is not essential to maintain the heat transfer rate of the condenser, because most of the heat flow occurs in the adjacent portions of the outer plate, which receives heat primarily from the metal tape surrounding the condenser tube [6, 7].

Figure 1 shows the location of the condenser skin in the cabinet body. The detail of the duct installation with tape is shown in Figure 2.

Few works have been found in the literature regarding the skin condenser concept. Some analyze the heat flow from the condenser tube to the external metallic plate of the cabinet, which transfers heat to the environment [7–14]. However, no publications have been found regarding the mechanism of noise generation caused by the pulsation of the gas discharge in the condenser. This paper analyzes this mechanism of noise generation in this concept of refrigerator.

2 Test in a refrigerator cabinet

To evaluate the vibration of the cabinet of a skin condenser, two refrigerators (A and B) of same model, positioned close to each other, were used. In one of them (refrigerator A) the complete refrigeration cycle was maintained,

*Corresponding author: ricardolschaefer@gmail.com

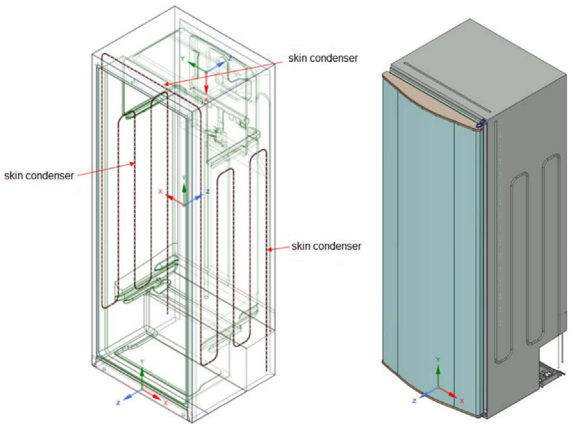

Figure 1. Refrigerator with skin condenser.

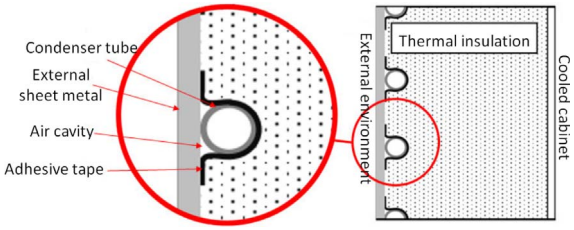

Figure 2. Detail of the skin condenser tube [8].

except for the condenser. For this, the discharge tube at the compressor outlet was connected to the condenser inlet of refrigerator B and its outlet was connected to refrigerator A. Figure 3 shows the front view of a schematic of the setup of this experiment. The cabinet dimension is 170 cm high, 62 cm wide and 70 cm deep, approximately. In order to avoid structural transmission of vibration between the refrigerators, flexible tubing was used in the suction and discharge tubes connecting the two equipments. In this way, the cabinet of refrigerator B was excited by pulsation only of the discharge gas, avoiding interference from other vibration sources.

Vibration measurement at one side wall of the cabinet was measured at 385 points by a laser vibrometer Polytec PSV-500. To increase the cooling cycle time, electrical resistances were used in refrigerator A, allowing vibration measurement on refrigerator B in longer stable condition.

The spectrum of the spatial average vibration of refrigerator cabinet B is shown in Figure 4. It shows peaks at the harmonics of the compressor operating frequency, but with varying amplitudes indicating that can excite vibrations with higher amplitudes at some harmonics compared to others (red vertical lines on the graph).

A continuous spectrum of the cabinet response in the 100–400 Hz range is also observed, indicating an additional vibration generation mechanism, but of less importance compared to that of the pulsating characteristics. Additional tests were performed on segments of the cabinet side wall in order to understand this vibration excitation mechanism in more detail.

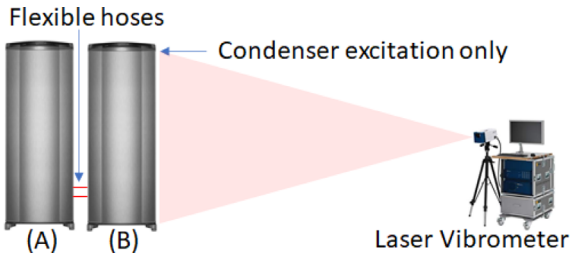

Figure 3. Representation of the cabinet side vibration mapping test.

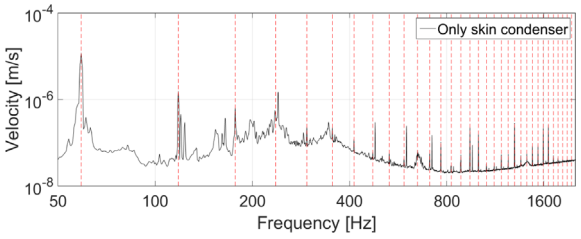

Figure 4. Vibration in the cabinet side only with skin condenser.

3 Tests on cabinet segments

The segments were composed of a steel plate (0.5 mm thickness), steel tube (external diameters of 5 mm and internal diameters of 4 mm) and a rigid polyurethane (PUR) body (250 mm), reproducing the wall structure of a typical refrigerator. The representation of the cabinet structure by segments of smaller dimensions facilitates the observation of the effect of pulsation harmonics on its dynamic behavior. The segments were manufactured in a refrigerator factory and this condition was essential to ensure the quality and homogeneity of the materials and manufacturing process.

Figure 5 shows a segment fabricated for these tests. Three configurations were fabricated: (I) straight condenser tube near the metal surface, (II) curved tube near the metal surface, and (III) straight tube in the middle of the PUR. Figure 6 shows the different configurations assembled.

A test set up was developed consisting of a refrigerator, a temperature and pressure measurement system (static and dynamic), and a support for the segments (Fig. 7).

The refrigerator was the source of pulsation which was transmitted to the segments through flexible tubes in order to avoid transmission of structural vibration. The measurement system provided the parameters monitoring to verify the stability of the cooling cycle.

Vibration was mapped with a laser vibrometer, which allowed measurements in the surface of each segment at 341 points and visualizing their vibration modes. Electrical resistors were installed inside the cabinet, increasing the cooling cycle period which allowed all points vibration measurements to be performed in a single and longer cycle after an initial stabilization period.

Figure 5. Example of segment (III) produced for bench test.

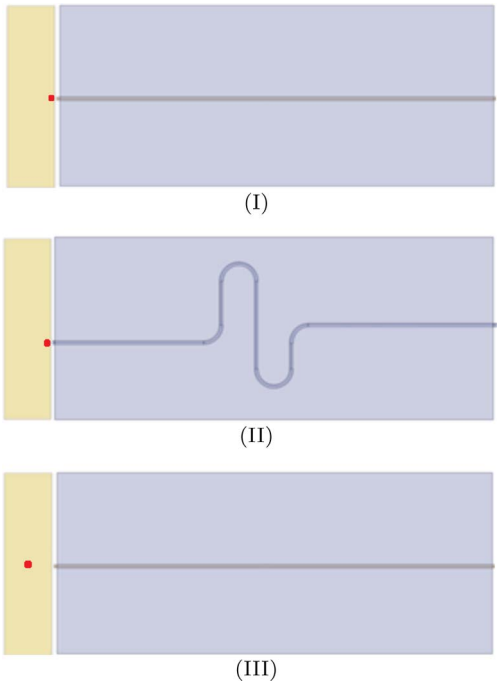

Figure 6. Geometries and position of the tube installed in the segments. The red dot indicates the tube position.

The spectra of the average vibration of all points on each segment are shown in Figure 8. They are very similar, indicating that the dynamic behavior of the analyzed segments depends mainly on the pulsation spectrum and are little influenced by the tube geometry or position in the mounting configuration.

The resultant of the vibration modes of the segments resemble their bending modes, which dominate the spectrum at low frequencies. Figures 9–11 show the vibrations mapped at the pulsation first harmonics: 59, 118, 177, 236, 295 and 354 Hz.

The results show that the segments vibration modes at the pulsation harmonics are very similar, despite their different geometries (curved and straight) and position (shallow and buried in the PUR) of the tube.

Given the proximity of the discharge tube to the metal plate it would be expected to observe greater amplitudes of vibration of the segment in this region, resulting from forced response of the plate due to deformation of the tube caused by internal pressure. However, this localized response was not visible by the mapping obtained.

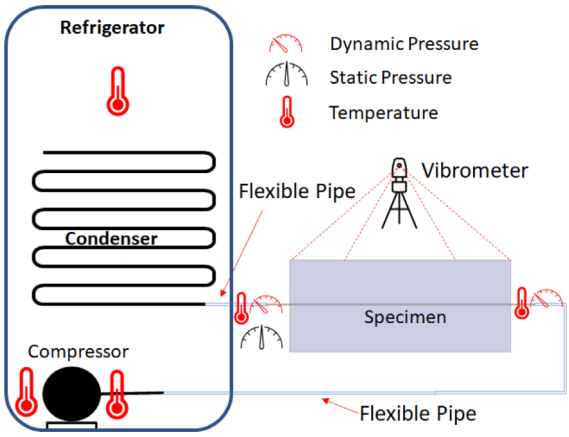

Figure 7. Bench developed for testing with segments.

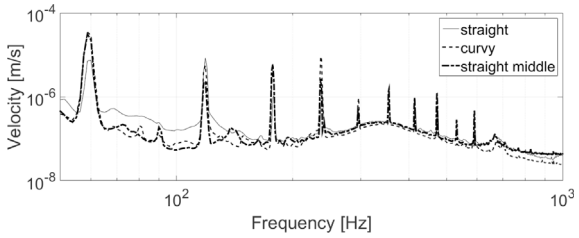

Figure 8. Spectra of the spatial averaging of vibrations in pulsation excited segments.

It is observed that the greatest responses occur at the pulsation harmonics and the segments vibrate in their own normal modes, whose resonant frequencies are close to some harmonics.

It is concluded that the deformation of the tube provides a distributed excitation on each segment and they vibrate in their own structural modes. The possible natural modes of the tube and the bending vibration generation mechanism caused by the internal pressure in the tube will be analyzed in the next section.

4 Bending modes in tubes excited by internal pressure

Analyses by finite elements (FEM) were performed to understand the effect of internal pressure in tubes. The tube was divided circumferentially into 24 and longitudinally into 200 solid elements with identical properties. The first analysis consisted of calculating the deflection in tubes with axisymmetric cross sections excited by a uniform pulsating internal pressure (free–free condition). The lateral deflection was chosen as an analysis parameter because it better indicates vibrations in bending modes. The amplitude of wall vibration in the radial direction for a steel tube with inner radius 4 mm, outer radius 5 mm and length 600 mm subjected to a uniform and unitary internal pressure is shown in Figure 12 for points at 0.3 L and 0.5 L, where L is the length of the tube.

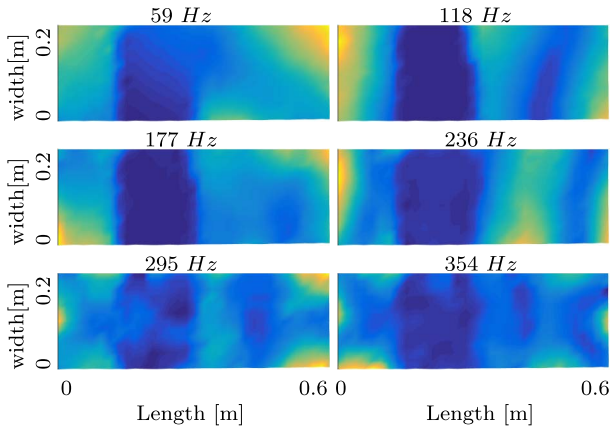

Figure 9. Operational deflection shapes for pulsation frequencies of the segment with straight tube on the surface (Fig. 6.I).

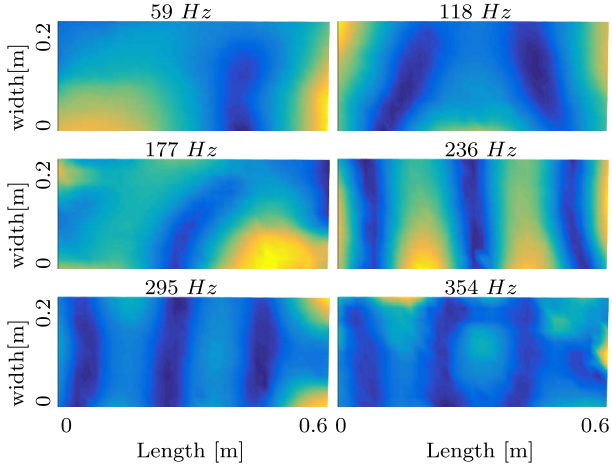

Figure 10. Operational deflection shapes for the pulsation frequencies of the segment with curved tube on the surface (Fig. 6.II).

The response spectrum indicates a peak at the frequency corresponding to the first axial resonant mode at 4.2 kHz and no excitation of bending modes. The first circumferential mode is outside this frequency range. The first radial mode is at 2.6 kHz, but is not evident due to the geometry of the tube, which has high radial stiffness even at its natural frequency.

Thus, based on the results shown in Figure 12, it can be stated that the internal pressure does not excite bending modes for tubes with symmetry in the cross section and the radial displacement will be proportional to the internal pressure, except the axial natural frequencies. Based on this, it was analyzed the effect on tubes with asymmetries. A new simulation was performed, with the deflection calculated for two situations: (1) symmetrical tube and (2) tube with segments with different material properties, as shown in Figure 13.

Results are shown in Figure 14, where it can be seen that the radial deflections of the asymmetric tube in longitudinal sections are similar to the deflections of the

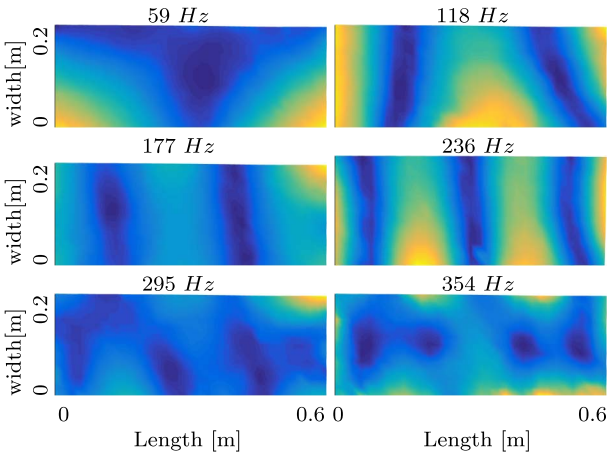

Figure 11. Operational deflection shapes for pulsation frequencies of segment with straight tube in the middle (Fig. 6.III).

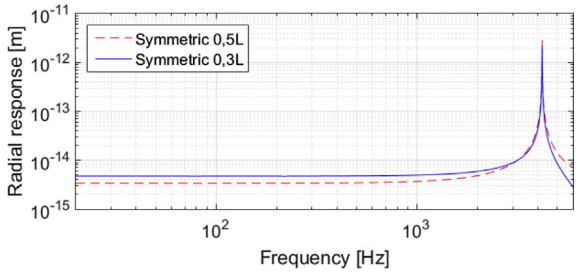

Figure 12. Radial response of a tube with symmetrical characteristics, excited by unitary internal pressure.

symmetric cross section tube. The asymmetric tube in longitudinal sections does not excite also bending modes, provided the cross section axial symmetry is preserved.

A further investigation was performed with variations in the tube cross section. The configuration of the asymmetry generated in the tube can be seen in Figure 15, where the upper part of the tube has slightly lower thickness.

The results of the calculated deflections, with unit internal pressure excitation, for all points over the length of the symmetric tube can be seen in Figure 16 and for the asymmetric tube in Figure 17.

Figures 16 and 17 show that the deflection of the asymmetric tube is higher at all frequencies. Thus, it is evident that the bending modes are excited due to the asymmetry in the cross section, which acts as a mechanism where small asymmetries are sufficient to induce flexural deflection.

Regarding the shape of the frequency response curves, it can be observed that only the odd bending modes were excited, and this becomes clear by the calculated deflection, shown in Figure 18, which also shows the receptance curve for a point force excitation at the end of the tube. It is observed that the internal pressure excites only the odd modes of the asymmetric tube.

The shape of the spectrum of the asymmetric tube, indicates a bending moment excitation. To show this, the deflection of the same tube was calculated when excited

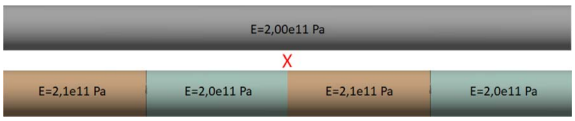

Figure 13. Comparison performed between the symmetrical tube and the tube with different modulus of elasticity in longitudinal sections.

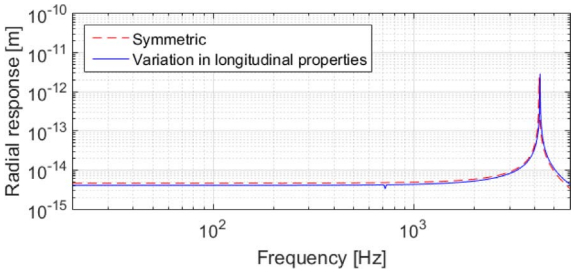

Figure 14. Calculated deflection at the point at 0.3 L of the symmetric and asymmetric tube in the longitudinal sections, excited by unit internal pressure.

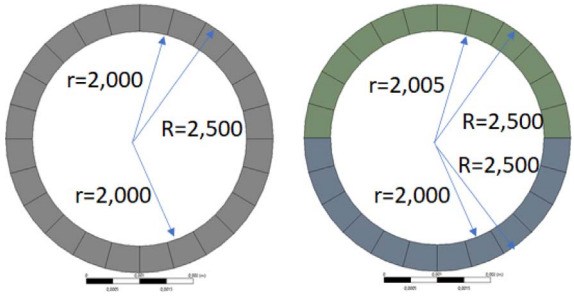

Figure 15. Geometric configuration of symmetric and asymmetric tubes.

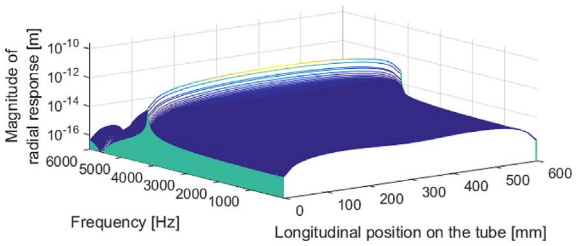

Figure 16. Deflection in a symmetric tube, excited by unitary internal pressure.

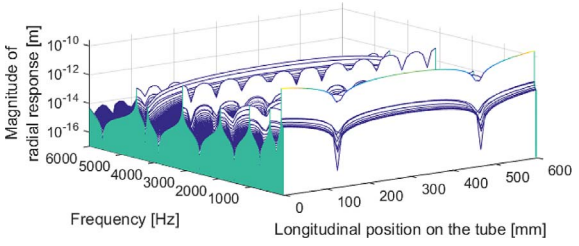

Figure 17. Deflection in an asymmetric tube, excited by unitary internal pressure.

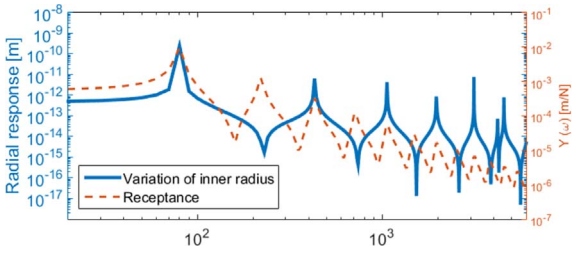

Figure 18. Deflection at the end point of the asymmetric tube excited by unitary internal pressure and point receptance excited by unitary force at the end of tube.

by unit internal pressure and by a unit bending moment applied at both ends. The results of the deflections are shown in Figure 19, where it can be seen that the spectra are identical at low frequencies and coincident in all excited modes except for the frequency of 4.2 kHz, which is the first axial mode.

The asymmetry in the tube cross section generates bending moment. An analysis was carried out considering the effects of stress and strain generated by pressure pulsation. The internal pressure generates stresses in the tube wall, and the axial stress (σ_{zz}) was calculated by Equation (1) [15]:

$$\sigma_{zz} = \frac{2\nu P_0 a^2}{(b^2 - a^2)} \ , \tag{1}$$

where P_0 is the internal pressure, a is the inner radius, b is the outer radius, and ν is Poisson's coefficient.

Therefore, the axial strain generated in symmetric cross section tubes will be equal at any circumferential point. However, in asymmetric tubes, the axial strain will not be uniform, as represented in Figure 20.

The difference between the deformations of the upper and lower parts causes a bowing shape in the tube, as shown in Figure 21.

The resultant forces are proportional to the cross sectional area and the axial stresses generated. The bending moment can be calculated by multiplying the lower and upper resultant forces by their respective distances from the centroid of the cross section to the neutral axis:

$$M = F_{u,l}\overline{y_{u,l}} \ , \tag{2}$$

in which $F_{u,l}$ is the upper or lower resultant force and $\overline{y_{u,l}}$ is the distance from the centroid of each half to the neutral axis.

The bending moment is related to the tube deflection by the following equation:

$$M = EI_s \frac{\partial^2 v(z)}{\partial z^2}, \tag{3}$$

in which I_S is the moment of inertia of the cross sectional area, E is the elasticity modulus and $v(z)$ is the deflection.

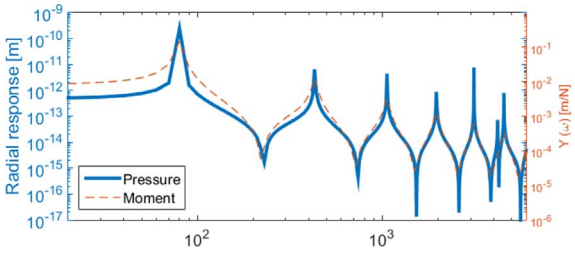

Figure 19. Deflection at the end of the asymmetric tube excited by pressure and bending moment.

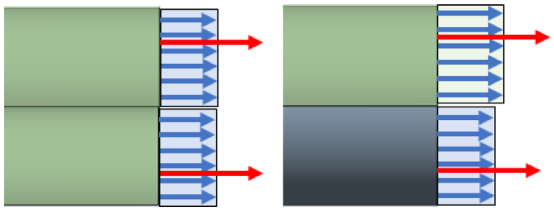

Figure 20. Representation of axial stress generated in symmetrical and asymmetrical tubes excited by internal pressure.

Considering Euler–Bernoulli Theory the flexural wave equation is given by [16]:

$$\frac{\partial^4 v(z,t)}{\partial z^4} - k^4 v(z,t) = 0; \tag{4}$$

where k is the bending wave number defined by:

$$k = \sqrt[4]{\frac{\omega^2 m'}{EI_s}}, \tag{5}$$

ω is the frequency (rad/s) and m' is the mass per unit length.

The solution can be given by [16]:

$$v(z,t) = \left(Ae^{jkz} + Be^{-jkz} + Ce^{kz} + De^{-kz}\right)e^{j\omega t}, \tag{6}$$

where A, B, C, and D are constants to be determined through boundary conditions.

For the free–free condition, the shear force at the ends is zero ($V_{0,L} = 0$) and the moment is equal to the generated bending moment ($M_{0,L} = M_0$). Applying the boundary conditions and arranging in matrix form:

$$\begin{bmatrix} -k^2 & -k^2 & k^2 & k^2 \\ -jk^3 & jk^3 & k^3 & -k^3 \\ -k^2 e^{jkL} & -k^2 e^{-jkL} & k^2 e^{kL} & k^2 e^{-kL} \\ -jk^3 e^{jkL} & jk^3 e^{-jkL} & k^3 e^{kL} & -k^3 e^{-kL} \end{bmatrix} \begin{Bmatrix} A \\ B \\ C \\ D \end{Bmatrix} = \begin{Bmatrix} \frac{M_0}{EI} \\ 0 \\ \frac{M_0}{EI} \\ 0 \end{Bmatrix}, \tag{7}$$

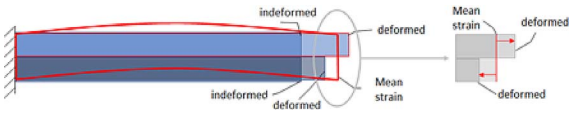

Figure 21. Bending deformation caused in a tube with asymmetry in the cross section.

the constants A, B, C and D are determined by solving the matrix system for each frequency, and the deflection can then be calculated by Equation (6).

Simulations were performed by FEM to validate the developed equations. The geometry of the numerical models were based on typical condenser tubes: length of 600 mm, external radius of 5 mm and internal radius of 4 mm. Three types of asymmetry were tested: (1) geometric, (2) modulus of elasticity, and (3) Poisson's coefficient. The mesh was generated with 12 elements in each half cross section, which assumed different values of thickness, modulus of elasticity, and Poisson's ratio in each of the configurations tested. Figure 22 shows the mesh used in the simulations.

To generate asymmetry in the geometry, the thickness of the elements in the upper half of the tube was considered 0.495 mm and those the lower half were 0.500 mm (Fig. 15).

The analytical calculation considering a bending moment given by Equation (2), was applied concentrated at each end. The analysis of the results in Figure 23 indicates good agreement throughout the spectrum.

To generate asymmetry in the modulus of elasticity, a different value was set for each element. For the elements in the upper half 2.001×10^{11} Pa was considered and 2.000×10^{11} for the elements of the lower half. Figure 24 shows a comparison between the results, indicating good agreement.

The simulation with different Poisson's ratio of the elements resulted in similar results, indicating that the same mechanism acts in the generation of bending moment in the tube.

The analyses performed on tubes with asymmetries in the cross section clearly show the excitation of vibration in bending modes caused by internal pressure, even if uniformly distributed along the tube inner wall. This mechanism provides a distributed excitation on the structural component. The structure responds at its natural frequency closest to that of the internal pressure and with a mode shape of its respective natural mode of vibration.

It is concluded that this mechanism of excitation of bending modes can also occur in tubes even with perfect geometric symmetry of cross section and material properties, but with assemblies that offer asymmetry in contacts with the structure. This is typically the case for the tubes of skin condensers which are in contact with the sheet metal along a line only and a fraction of their outer surface in contact with the thermal insulator of the cabinet wall, as shown in Figure 2. This mounting asymmetry is sufficient to induce bending vibration.

It should also be remembered that tube manufacturing processes result in cross sections with slight geometric asymmetries and variations in material properties, despite

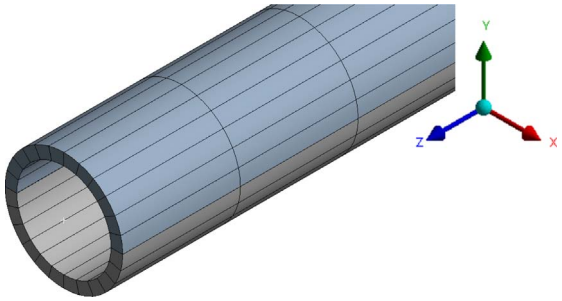

Figure 22. Discretization used for the asymmetric tube.

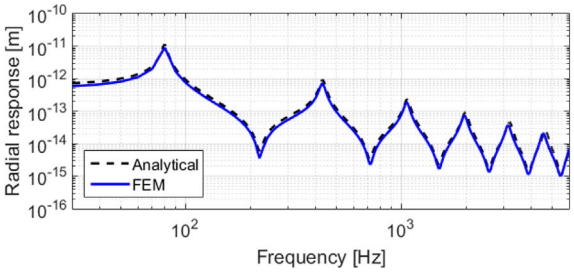

Figure 23. Comparison of numerically and analytically calculated deflections at one end for thickness asymmetrical tube.

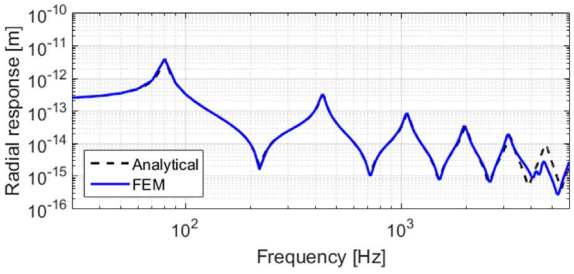

Figure 24. Comparison of numerically and analytically calculated deflections at one end for modulus of elasticity asymmetrical tube.

small they may be. Considering the asymmetries arising from the assembly of the tubes, the excitation of vibration in bending modes is inevitable. This mechanism explains why the vibrations measured in the segments indicated the forms of their natural modes and not only the region of the plate located in contact with the tube, as would be expected in first place if the tube presented only pulsating vibration modes.

5 Conclusions

The experimental and theoretical analyses performed became possible to understand the mechanism of transformation of the pulsation energy into vibration, which is transmitted to the cabinet structure.

The experimental results showed that the segments and the cabinet, when excited only by gas pulsation, vibrate mainly in bending modes. Thus, the natural axial, radial and circumferential modes of the tube do not show representative effects when excited by pulsation and their effects can be considered secondary in analyses of tubes with geometries such as those used in this work.

It was possible to determine the amplitude of the deformation of the tubes when excited by internal pressure. The results found were similar to those found by finite element which validates the analysis.

With regard to practical application, the phenomenon described has relevance in long tubes and small diameters, where the natural bending modes will be predominant at low frequencies, which is also the most important range for pulsation.

Conflict of interest

The authors declare that there is no conflict of interest.

Acknowledgments

The authors thank UFSC and UNIOESTE.

References

1. J.Y. Jeon, J. You, H.Y. Chang: Sound radiation and sound quality characteristics of refrigerator noise in real living environments. Applied Acoustics 68 (2006) 1118–1134.
2. H. Koruk, A. Arisoy: Identification of crack noises in household refrigerators. Applied Acoustics 89 (2015) 234–243.
3. H.K. Lee, J.S. Park, K.B. Hur: The radiation of the noise/vibration generated by the discharge valve system in hermetic compressor for refrigerator, in International Compressor Engineering Conference, West Lafayette, IN, USA, July 25–28, 2000. Purdue University. Paper 1438.
4. J.C. Wachel, J.D. Tison: Vibrations in recirpocating machinery and piping systems. Engineering Dynamics Incorporated Seminar Manual, San Antonio, TX, 1999.
5. C.C.S. Dall'Alba, F.T. Knabben, R.S. Espíndola, C.J.L. Hermes: Heat transfer interactions between skin-type condensers and evaporators and their effect on the energy consumption of dual-skin chest-freezers. Applied Thermal Engineering 183 (2021) 2.
6. N. Ghule, S.D. Mahajan: Mathematical modeling of skin condensers for domestic refrigerator. International Journal of Mechanical and Industrial Technology 3 (2015) 102–115.
7. A.D. Rayiani, N.R. Sheth, N.C. Niraj: Thermal analysis of hot-wall condenser for domestic refrigerator. IJSR 3, 7 (2014) 622–626.
8. R.S. Espíndola: Theoretical and experimental analysis of the performance of household refrigerators running with hot-wall condensers. MEng thesis, Federal University of Santa Catarina, Florianopolis, SC, Brazil, 2017.
9. E.G. Colombo, R.S. Espíndola, F.T. Knabben, C. Melo: A numerical and experimental investigation on skin condensers applied to household refrigerators, in Int. Conf. Refrigeration and Air Conditioning, West Lafayette, IN, USA, July 11–14, 2016. Purdue University. Paper 1583.
10. R.S. Espíndola, F.T. Knabben, C. Melo, C.J.L. Hermes: Thermal performance of skin-type, hot-wall condensers, part-I: component-level modeling and experimental evaluation. International Journal of Refrigeration 110 (2020) 231–238.

11. R.S. Espíndola, F.T. Knabben, C. Melo, C.J.L. Hermes: Thermal performance of skin-type, hot-wall condensers, part-II: Design guidelines for household applications. International Journal of Refrigeration 110 (2020) 262–267.
12. P.K. Bansai, T.C. Chin: Design and modeling of hot-wall condensers in domestic refrigerators. Applied Thermal _Engineering 22, 14 (2002) 1601–1617.
13. A. Rebora, L.A. Tagliafico: Thermal performance analysis for hot-wall condenser and evaporator configurations in refrigeration appliances. International Journal of Refrigeration 21, 6 (1997) 490–502.
14. J.K. Gupta, M.R. Gopal: Modeling of hot-wall condensers for domestic refrigerators. International Journal of Refrigeration 31, 6 (2008) 979–988.
15. J.R. Barber: Intermediate Mechanics of Materials. Springer, 2010.
16. K.F. Graff: Wave Motion in Elastic Solids. Oxford University Press, 1975.

Cite this article as: Schaefer RL. & Lenzi A. 2022. Excitation of pipe bending modes by internal pressure: A phenomenon present in refrigerators with skin condenser. Acta Acustica, **6**, 35.